Annihilating Dark Matter Search with 12 Years of Fermi LAT Data in Nearby Galaxy Clusters

C. Thorpe-Morgan[1*], D. Malyshev[1], C-A. Stegen[1], A. Santangelo [1] and J. Jochum [1]

1 Institut für Astronomie und Astrophysik Tübingen, Tübingen, Germany
* charles.thorpe-morgan@astro.uni-tuebingen.de

October 4, 2022
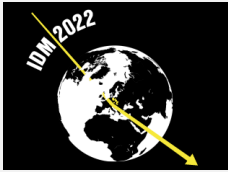
Abstract

Galaxy clusters contain an abundance of dark matter making them attractive laboratories for indirect DM searches. This work details a search for signals of pair annihilation from WIMP dark matter in the GeV gamma ray regime in five low z and high galactic latitude galaxy clusters (Centaurus, Coma, Virgo, Perseus and Fornax); undertaken using nearly 12 years of Fermi/LAT data. Through the non-detection of this characteristic signal, we derive constraints on the annihilation cross-section of DM pair annihilation into the $b\bar{b}$, W^+W^- and $\gamma\gamma$ channels. The limits obtained are of a comparable magnitude to those of recently derived from Fermi/LAT observations of dwarf spheroidal galaxies.

1 Introduction

Dark Matter (DM) is among the greatest unknowns of modern physics and cosmology, it poses a significant challenge to our current interpretation of the universe and after decades of research little is still known about its physical properties. Weakly Interacting Massive Particles (WIMPs) continue to be a favoured theory of DM for several reasons. Firstly, WIMPS of annihilation cross-section around the weak scale naturally produce a relic density of dark matter of the same order seen today (the so-called WIMP miracle) [1,2], see [3,4] for pedagogical reviews. Crucially however, WIMPS remain achievable to test through direct and indirect detection methods. Their expected decay to standard model (SM) particles allows the production of primary and secondary photons that form an excess on top of astrophysical foregrounds. This study aimed to detect such an excess in five nearby galaxy clusters, originating from pair annihilation of GeV scale WIMP dark matter, using the Fermi/LAT instrument.

Galaxy clusters as objects are the largest gravitationally bound systems in the universe. Their resulting high masses therefore give rise to an abundance of DM located within them, in turn making them promising objects to derive competitive limits on the properties of WIMP DM. The extensive study of clusters kinematics (derived from both strong and weak lensing surveys [5] (and references therein) as well as generally low astrophysical foregrounds in the GeV energy range make them advantageous targets. However occasional coincident bright sources within clusters as well as uncertainties surrounding their mass profiles can dampen the potential of these objects.

2 Signal and Galaxy Clusters sample

2.1 Dark Matter Signal

The production of SM particles (here denoted as $f\bar{f}$) from a DM annihilation event is given by: $\chi\bar{\chi} \to f\bar{f}$. Accordingly, the spectrum of gamma ray radiation from annihilation within a DM dominated object of solid angle $d\Omega$, follows the form: see e.g. [6]

$$\frac{dF(E)}{d\Omega} \equiv \frac{dN_\gamma}{dEd\Omega} = \frac{dJ/d\Omega}{4\pi \cdot 2m_{DM}^2} \times \sum_f b_f \cdot \langle\sigma_f v\rangle \cdot \frac{dN_\gamma^f}{dE}(E) \tag{1}$$

Here m_{DM} is the mass of the DM particle χ, J is the object's J-factor, a term given by the integral of DM density ρ square over the line of sight:

$$dJ/d\Omega = \int_{l.o.s} \rho^2(\ell)d\ell \tag{2}$$

The first half of this product represents the contributions from astrophysics (specifically the sum of the DM annihilations in the line of sight), where the second half corresponds to the spectrum of a single annihilation event (encompassing particle physics factors). In the latter, the branching ratio is denoted by b_f and represents the likelihood of the annihilation event producing a given SM product, where $\sum_f b_f = 1$. dN_γ^f/dE is the spectrum produced from a single annihilation event into a given channel. Critical to the derivation of limits is the dark matter velocity averaged annihilation cross-section, here given as $\langle\sigma_f v\rangle$ (in the $f\bar{f}$ channel).This study utilised the assumption of an 100% branching ratio into each investigated channel, the terms in the equation however have been left in for posterity.

Inspection of this equation reveals a given annihilation signal's strength is strongly dependent on the J-factor (itself dependent of the square of the dark matter density) and the $\langle\sigma_f v\rangle$ term. Astrophysical objects (such as galaxy clusters) with high dark matter densities therefore maximise the J-factor's quadratic dependence upon density providing the potential for strong signals from DM annihilation.

2.2 Cluster Sample

In order to maximise the J-factor of our cluster sample, we utilised clusters that both had minimal distances ($z \lesssim 0.02$), as well as a high galactic latitude and a lack of central bright GeV sources to avoid complications associated with the bright GeV emission of the galactic plane and objects internal to the galaxy clusters. The targets selected included the Centaurus, Coma, Virgo, Perseus and Fornax clusters (this sample overlaps in part with the previous study [7]), and for each of these clusters dark matter profiles reported in literature were utilised; as described in Table 1 .

2.3 Dark Matter Distribution

The strong quadratic dependence of the J-factor on the DM density distribution demanded the study utilised dark matter density profiles that accurately described the profiles of each cluster in the sample. To this end, we implemented a generalised NFW (Zhao [8]) profile for each cluster to accurately describe this, given by:

$$\rho(r) = \frac{2^{\frac{\beta-\gamma}{\alpha}} \rho_s}{(\frac{r}{r_s})^\gamma (1 + (\frac{r}{r_s})^\alpha)^{(\beta-\gamma)/\alpha}} \tag{3}$$

$$\text{with } \alpha = 1; \quad \beta = 3; \quad \gamma = 1$$

a spherically symmetric equation describing the density of dark matter as a function of distance (r) from the object's centre. Quoted below the equation are also the α, β and γ values that, with $\rho_0 = 4\rho_s$, return the original NFW profile [9]. The characteristic DM density ρ_s and scale radius r_s are values that are individual to each object and the values adopted for each cluster are described in the Table 1 in Appendix A along with the references to works which provide the sources of these values.

In addition to to the aforementioned profiles from literature, this study made use of the CLUMPY v.3 code [10–12] to derive the radial dependence of each cluster's J-factor. The utilisation of the CLUMPY code also allowed the additional opportunity to consider the effect of substructure in each cluster's profile, namely this is the hierarchical formation of smaller clumps of dark matter seen in cold dark matter cosmological N-body simulations   see e.g [13,14], such substructures can provide a significant boost to the overall annihilation signal. For each cluster where substructures were applied, we use a mass distribution function of $dN_{sub}/dM \propto M^{-1.9}$ where a 10% mass fraction is in substructures [14],we also adopt a minimal/maximal substructure mass to be $10^{-6}/10^{-2} M_{clust}$ and followed the same protocol as within [15] with regards to the mass-concentration relation of the sub-clumps. We implemented that the spatial distribution of the substructures dN_{sub}/dV should follow the smooth profile of the associated cluster thus lending to a even boost of the J-factor and a stronger boost to the signal at greater radii.

The density profiles of all clusters were assumed to continue up to the largest distances from the center at which profile measurements were reported in the references in Tab. 1 (0.5 Mpc for Centaurus; 1 Mpc for the rest of the clusters). We note the possibility of the strong model dependence of the boosted signal thus present the results for both cases below – the halo with substructures ("boosted") and smooth halo only ("non-boosted") dark matter profiles.

3 Data Analysis

The gamma ray data utilised in this study were filtered to ensure only events with an energy range of 100 MeV to 300 GeV passing the P8R3_CLEAN_V2 cut [1] were considered for analysis. The study drew upon 12 years of survey mode data from the Fermi/LAT instrument, taken between the 4th August 2008 to the 23rd April 2020. Further cuts applied to this data set included standardised time cuts (as described in [16]) as well as cuts in the zenith angle - specifically $\theta < 100°$ - preventing erroneous categorisation of events from the Earth's albedo.

To implement a binned analysis we selected a region of a 15° radius around each cluster, furthermore enabling energy dispersion handling within the analysis of this region. The sources within each of these regions were then modelled using the 4FGL catalogue [17], sources from a further 10° outside the considered region were also considered but had their spectral parameters frozen. Diffuse emission templates gll_iem_v07.fits and iso_P8R3_CLEAN_V2_v1.txt were also implemented to account for galactic and extra-galactic diffuse emission respectively. For in-region sources and diffuse emission, we adopted the ap-

---

[1]See Fermi/LAT data analysis guidelines.
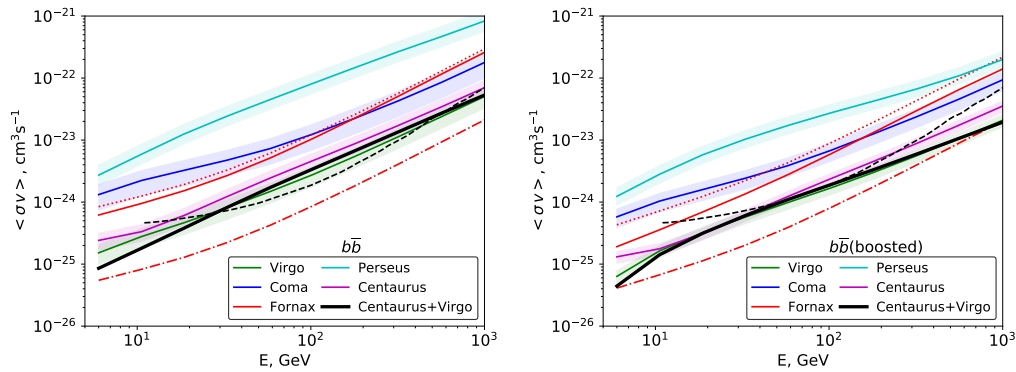
Figure 1: Limits produced by this work on the annihilation cross-section of DM annihilating into the $b\bar{b}$ from various galaxy clusters. Limits are presented at a 95% confidence level, additionally 1σ uncertainties are represented by shaded regions. The two panels show the effect of the omission (left) and inclusion of substructure (right) as described in the text.

proach of initially freeing their spectral parameters and performing a broadband fit, before fixing spectral parameters except normalisation to their best fit values.

After accounting for the astrophysical foreground, we included a template of spatial emission distributed following the cluster's J-factor. The spectral component of this differed with the selected annihilation channel and to account for this we implemented the fermitools `DMFitFunction` from [18] for both the $b\bar{b}$ and $W^{+}W^{-}$ channel. An alternative approach of assuming a Gaussian of 5% energy width was used for the $\gamma\gamma$ channel. This feature also required an alternative approach to the analysis, thus we instead performed a finer binned analysis with 50 energy bins per energy decade rather than the 10 per decade used previously. Due to the increase in computational demand, we only performed the search in this annihilation channel in the two clusters providing the most stringent limits in other channels (Virgo and Centaurus).

4   Results and Discussion

The study found no detection of DM at a level above $> 2.5\sigma$ from any of the clusters, however the absence of this detection allowed for the calculation of 95% C.L. on the annihilation cross section in the $b\bar{b}$ and $W^{+}W^{-}$ channel, both strongly motivated channels in the WIMP-minimal Supersymmetric Standard Models [18]. Limits on direct WIMP annihilation to the $\gamma\gamma$ channel were furthermore calculated in the Virgo and Centaurus clusters, given that they displayed the strongest limits in other channels. We present these limits in Fig. 1,2 and 3, where the limits in each channel are presented both with and without the presence of substructures in the DM profile (referred to here as boost).

Constraints were derived from reported density profiles of each considered cluster, the tightest constraints formally came from the RB02 [19] in the Fornax cluster (represented by red dot-dashed lines in Figs. 1–2). However, despite these strong limits we find that the other reported Fornax profiles (DW01 [20] and SR10A10 [21] solid and dotted red lines accordingly) report in considerably lower constraints (a factor of ~ 20). This discrepancy was also noted in a TeV study conducted by H.E.S.S. [22] and due to this reason we omit this profile from our final conclusions.

With this profile excluded, the clusters Virgo and Centaurus provide the best strongest

limits on the annihilation cross-section. Coma and Perseus, the remaining two investigated clusters, suffer from limits of up to an order of magnitude higher than their counterparts. Given the lower J-factor and bright sources associated with these two clusters, these less stringent limits are expected.

By building the log-likelihood profile of Virgo and Centaurus as a function of $\langle \sigma v \rangle$, we were able to combine their limits to perform a stacked analysis. In Figs 1–2, the solid black line represents the limits derived from these and corresponds to a $\langle \sigma v \rangle$ value at which the sum of log-likelihood profiles changes by 2.71/2 [23][2].

5   Conclusion

The limits presented in this work show the viability and potential of galaxy clusters in the field of indirect search for dark matter. Although weaker than limits derived from other sources of higher J-factors, the limits derived do remain comparable within an order of magnitude to other categories of object e.g. recent constraints pertaining from a stacked analysis of a many dwarf spheroidal galaxies [24,25]. We note also that the uncertainties associated with stacking large number of dwarf spheroidals with individual profiles that have high uncertainties can impact the total limits by a factor of 2 [26]. Though we note that systematic uncertainties in the DM density profiles of clusters can detrimentally impact the limits derived. Finally we argue that the limits derived from multiple different object types are fundamental to the search for dark matter, providing the cross-check quintessential for the confirmation of the nature of any detected signal.

Acknowledgements

The authors acknowledge support by the state of Baden-Württemberg through bwHPC.

Funding information   This work was supported by the DFG through the grant MA 7807/2-1

References

[1] B. W. Lee and S. Weinberg, *Cosmological lower bound on heavy-neutrino masses*, **39**(4), 165 (1977), doi:10.1103/PhysRevLett.39.165.

[2] J. L. Feng and J. Kumar, *Dark-Matter Particles without Weak-Scale Masses or Weak Interactions*, **101**(23), 231301 (2008), doi:10.1103/PhysRevLett.101.231301, 0803.4196.

[3] S. Profumo, *TASI 2012 Lectures on Astrophysical Probes of Dark Matter*, arXiv e-prints arXiv:1301.0952 (2013), 1301.0952.

[4] H. Baer, K.-Y. Choi, J. E. Kim and L. Roszkowski, *Dark matter production in the early universe: Beyond the thermal wimp paradigm*, Physics Reports **555**, 1–60 (2015), doi:10.1016/j.physrep.2014.10.002.

[5] S. Bhattacharya, S. Habib, K. Heitmann and A. Vikhlinin, *Dark Matter Halo Profiles of Massive Clusters: Theory versus Observations*, **766**(1), 32 (2013), doi:10.1088/0004-637X/766/1/32, 1112.5479.

---

[2]See also discussion on Fermi/LAT upper limits calculation.

[6] M. Cirelli, G. Corcella, A. Hektor, G. Hütsi, M. Kadastik, P. Panci, M. Raidal, F. Sala and A. Strumia, *PPPC 4 DM ID: a poor particle physicist cookbook for dark matter indirect detection*, **2011**(3), 051 (2011), doi:10.1088/1475-7516/2011/03/051, 1012.4515.

[7] X. Huang, G. Vertongen and C. Weniger, *Probing dark matter decay and annihilation with fermi lat observations of nearby galaxy clusters*, Journal of Cosmology and Astroparticle Physics - JCAP **2012** (2011), doi:10.1088/1475-7516/2012/01/042.

[8] H. Zhao, *Analytical models for galactic nuclei*, **278**(2), 488 (1996), doi:10.1093/mnras/278.2.488, astro-ph/9509122.

[9] J. F. Navarro, C. S. Frenk and S. D. M. White, *A universal density profile from hierarchical clustering*, The Astrophysical Journal **490**(2), 493–508 (1997), doi:10.1086/304888.

[10] A. Charbonnier, C. Combet and D. Maurin, *CLUMPY: A code for γ-ray signals from dark matter structures*, Computer Physics Communications **183**(3), 656 (2012), doi:10.1016/j.cpc.2011.10.017, 1201.4728.

[11] V. Bonnivard, M. Hütten, E. Nezri, A. Charbonnier, C. Combet and D. Maurin, *CLUMPY: Jeans analysis, γ-ray and ν fluxes from dark matter (sub-)structures*, Computer Physics Communications **200**, 336 (2016), doi:10.1016/j.cpc.2015.11.012, 1506.07628.

[12] M. Hütten, C. Combet and D. Maurin, *CLUMPY v3: γ-ray and ν signals from dark matter at all scales*, Computer Physics Communications **235**, 336 (2019), doi:10.1016/j.cpc.2018.10.001, 1806.08639.

[13] J. Diemand, M. Kuhlen and P. Madau, *Dark Matter Substructure and Gamma-Ray Annihilation in the Milky Way Halo*, **657**(1), 262 (2007), doi:10.1086/510736, astro-ph/0611370.

[14] V. Springel, J. Wang, M. Vogelsberger, A. Ludlow, A. Jenkins, A. Helmi, J. F. Navarro, C. S. Frenk and S. D. M. White, *The aquarius project: the subhaloes of galactic haloes*, Monthly Notices of the Royal Astronomical Society **391**(4), 1685–1711 (2008), doi:10.1111/j.1365-2966.2008.14066.x.

[15] M. A. Sánchez-Conde and F. Prada, *The flattening of the concentration-mass relation towards low halo masses and its implications for the annihilation signal boost*, **442**(3), 2271 (2014), doi:10.1093/mnras/stu1014, 1312.1729.

[16] W. B. Atwood, A. A. Abdo, M. Ackermann, W. Althouse, B. Anderson, M. Axelsson, L. Baldini, J. Ballet, D. L. Band, G. Barbiellini and et al., *The large area telescope on the fermi gamma-ray space telescopemission*, The Astrophysical Journal **697**(2), 1071–1102 (2009), doi:10.1088/0004-637x/697/2/1071.

[17] S. Abdollahi, F. Acero, M. Ackermann, M. Ajello, W. B. Atwood, M. Axelsson, L. Baldini, J. Ballet, G. Barbiellini, D. Bastieri, J. Becerra Gonzalez, R. Bellazzini *et al.*, *Fermi Large Area Telescope Fourth Source Catalog*, **247**(1), 33 (2020), doi:10.3847/1538-4365/ab6bcb, 1902.10045.

[18] T. E. Jeltema and S. Profumo, *Fitting the gamma-ray spectrum from dark matter with DMFIT: GLAST and the galactic center region*, **2008**(11), 003 (2008), doi:10.1088/1475-7516/2008/11/003, 0808.2641.

[19] T. H. Reiprich and H. Bohringer, *The mass function of an x-ray flux–limited sample of galaxy clusters*, The Astrophysical Journal **567**(2), 716–740 (2002), doi:10.1086/338753.

[20] M. J. Drinkwater, M. D. Gregg and M. Colless, *Substructure and Dynamics of the Fornax Cluster*, **548**(2), L139 (2001), doi:10.1086/319113, astro-ph/0012415.

[21] Y. Schuberth, T. Richtler, M. Hilker, B. Dirsch, L. P. Bassino, A. J. Romanowsky and L. Infante, *The globular cluster system of NGC 1399. V. dynamics of the cluster system out to 80 kpc*, **513**, A52 (2010), doi:10.1051/0004-6361/200912482, 0911.0420.

[22] A. Abramowski, F. Acero, F. Aharonian, A. G. Akhperjanian, G. Anton, A. Balzer, A. Barnacka, U. Barres de Almeida, Y. Becherini, J. Becker and et al., *Search for dark matter annihilation signals from the fornax galaxy cluster with h.e.s.s.*, The Astrophysical Journal **750**(2), 123 (2012), doi:10.1088/0004-637x/750/2/123.

[23] W. A. Rolke, A. M. López and J. Conrad, *Limits and confidence intervals in the presence of nuisance parameters*, Nuclear Instruments and Methods in Physics Research A **551**(2-3), 493 (2005), doi:10.1016/j.nima.2005.05.068, physics/0403059.

[24] M. Ackermann, A. Albert, B. Anderson, W. B. Atwood, L. Baldini, G. Barbiellini, D. Bastieri, K. Bechtol, R. Bellazzini, E. Bissaldi, R. D. Bland ford, E. D. Bloom *et al.*, *Searching for Dark Matter Annihilation from Milky Way Dwarf Spheroidal Galaxies with Six Years of Fermi Large Area Telescope Data*, **115**(23), 231301 (2015), doi:10.1103/PhysRevLett.115.231301, 1503.02641.

[25] S. Hoof, A. Geringer-Sameth and R. Trotta, *A global analysis of dark matter signals from 27 dwarf spheroidal galaxies using 11 years of Fermi-LAT observations*, **2020**(2), 012 (2020), doi:10.1088/1475-7516/2020/02/012, 1812.06986.

[26] T. Linden, *Robust method for treating astrophysical mismodeling in dark matter annihilation searches of dwarf spheroidal galaxies*, **101**(4), 043017 (2020), doi:10.1103/PhysRevD.101.043017, 1905.11992.

[27] S. Ettori, S. De Grandi and S. Molendi, *Gravitating mass profiles of nearby galaxy clusters and relations with X-ray gas temperature, luminosity and mass*, **391**, 841 (2002), doi:10.1051/0004-6361:20020905, astro-ph/0206120.

[28] R. Gavazzi, C. Adami, F. Durret, J. C. Cuillandre, O. Ilbert, A. Mazure, R. Pelló and M. P. Ulmer, *A weak lensing study of the Coma cluster*, **498**(2), L33 (2009), doi:10.1051/0004-6361/200911841, 0904.0220.

[29] D. E. McLaughlin, *Evidence in Virgo for the Universal Dark Matter Halo*, **512**(1), L9 (1999), doi:10.1086/311860, astro-ph/9812242.

[30] A. Simionescu, S. W. Allen, A. Mantz, N. Werner, Y. Takei, R. G. Morris, A. C. Fabian, J. S. Sanders, P. E. J. Nulsen, M. R. George and G. B. Taylor, *Baryons at the Edge of the X-ray-Brightest Galaxy Cluster*, Science **331**(6024), 1576 (2011), doi:10.1126/science.1200331, 1102.2429.

[31] T. H. Reiprich and H. Böhringer, *The Mass Function of an X-Ray Flux-limited Sample of Galaxy Clusters*, **567**(2), 716 (2002), doi:10.1086/338753, astro-ph/0111285.

A Appendix

Cluster	l [deg]	b [deg]	z	r_s [kpc]	ρ_s $[10^5 M/\text{kpc}^3]$	Reference
Centaurus	302.398	21.561	0.0114	470	2.13	[27]
Coma	283.807	74.437	0.0231	360	2.75	[28]
Virgo	187.697	12.337	0.0036	560	0.8	[29]
Perseus	150.573	-13.262	0.0179	369	2.73	[30]
Perseus	150.573	-13.262	0.0179	530	2.36	[27]
Fornax	236.712	-53.640	0.0046	220	1.25	[20](DW01)
Fornax	236.712	-53.640	0.0046	98	14.5	[31](RB02)
Fornax	236.712	-53.640	0.0046	34	22.0	[21](SR10A10)

Table 1: Tabulated details of the clusters investigated for DM annihilation signal in this work. Positional coordinates are presented in the galactic coordinate system (longitude - l and latitude - b). r_s and ρ_s are the characteristic radius and densities (Here, ρ_s corresponds to $\rho_0/4$ in an NFW profile) of the NFW Profile (see eq. 3) and their values are taken from the given references.
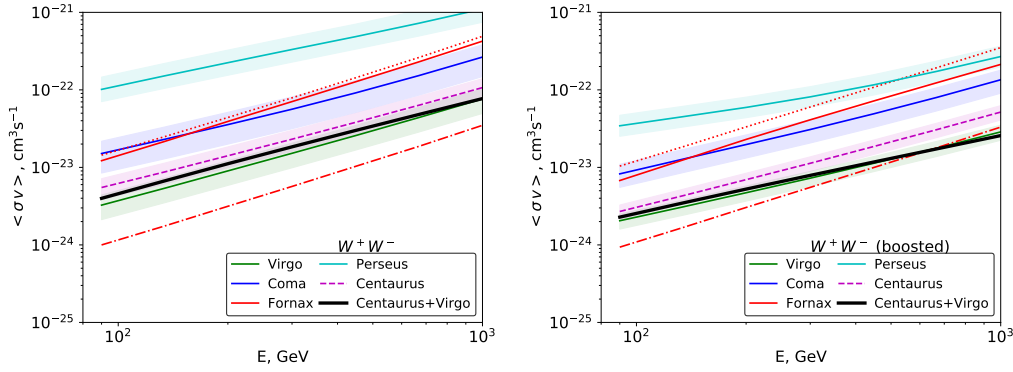
Figure 2: Limits on the annihilation cross-section of DM annihilating into the W^+W^- from various galaxy clusters at a 95% confidence level. See Fig. 1 for detailed panel and lines description.
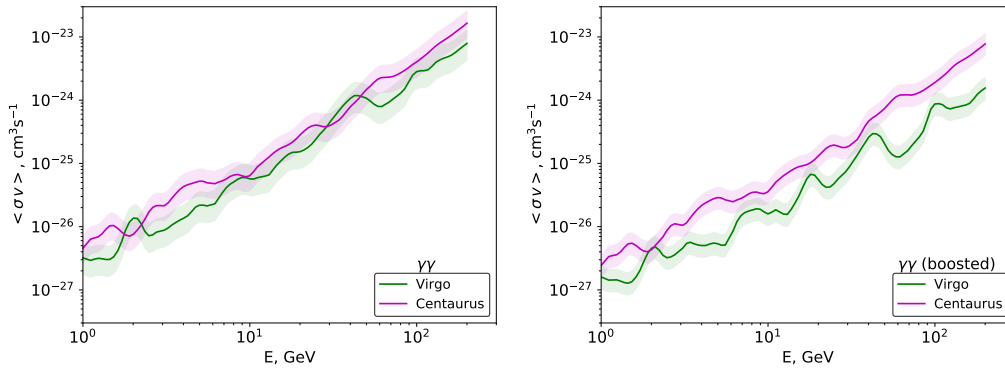
Figure 3: Limits produced from the $\gamma\gamma$ annihilation channel of WIMP DM at 95% confidence limit. Limits were only produced for the Virgo and Centaurus clusters given their superior constraints in other channels´. See Fig. 1 for detailed panel and lines description.